Mat. Res. Soc. Symp. Proc. Vol. 675 © 2001 Materials Research Society

Encapsulated Molecules in Carbon Nanotubes: Structure and Properties

Richard Russo, Brian W. Smith, B.C. Satishkumar, David E. Luzzi*

Laboratory for Research in the Structure of Matter
*Department of Materials Science and Engineering
University of Pennsylvania
3231 Walnut Street, Philadelphia, PA 19104-6272, USA

Harry C. Dorn

Department of Chemistry
Virginia Polytechnic Institute and State University
Blacksburg, Virginia 24061, USA

ABSTRACT

We encapsulate a number of fullerenes inside single-walled carbon nanotubes (SWNTs) including $La_2@C_{80}$ and $Er_xSc_{3-x}N@C_{80}$(x=0-3). The structural properties of these nanoscopic hybrid materials are described using high resolution transmission electron microscopy and electron diffraction. It is found that the encapsulated fullerenes self-assemble into long, one-dimensional chains. The thermal stability of these supramolecular assemblies are studied and large variations are found. The behavior is nominally consistent with the mass of the encapsulated metallofullerenes.

INTRODUCTION

Many future applications of single-walled carbon nanotubes (SWNTs) will depend upon the ability to modify their intrinsic properties by manipulating their structure. One novel means for modifying the properties of a SWNT is through the filling of its interior cavity with other molecules. For example, we have shown that "peapods," comprising SWNTs filled with 1-D chains of C_{60}, can be manufactured via a vapor phase and/or surface diffusion mechanism. This scalable process consists of annealing the sample in the presence of C_{60} at ~400°C. The presence of interior C_{60} is known to decrease the SWNT's compressibility [1] and has been shown by molecular dynamics simulation to increase its elastic modulus [2].

Our method of encapsulation has recently been extended to other related molecules, including the metallofullerenes $La_2@C_{80}$ and $Gd@C_{82}$. The case of $La_2@C_{80}@SWNT$ served as the first definitive proof that a non-intrinsic molecule could be inserted in bulk into SWNTs. In these experiments, it was directly observed by transmission electron microscopy (TEM) that the La atoms within the encapsulated C_{80} cages tumbled in a discontinuous motion [3], in direct conflict with the continuous motion detected by solution NMR experiments [4]. This was interpreted as the result of an interaction between the SWNT and the contained $La_2@C_{80}$ molecules, providing yet another

indication that interior molecules can modify the properties of a SWNT. In the case of $Gd@C_{82}$@SWNT, preliminary results indicate that the electrical resistance of a SWNT mat was affected by the presence of interior $Gd@C_{82}$ [5].

The present work involves a novel endohedral metallofullerene system, $Er_xSc_{3-x}N@C_{80}$ (x =0-3). This system comes with the ability to substitute several different metals in the nitrogen cluster, which will undoubtedly affect the charge transfer properties between the metal nitride cluster and the fullerene cage. These effects, when coupled with encapsulation in SWNTs, will create a series of hybrid materials with tunable electronic properties. In addition, a typical yield in the synthesis of metallofullerenes is 0.5%. It has been found that the yield of $Sc_3N@C_{80}$ is 3-5%. Unfortunately, the physical properties of these metallofullerenes, such as sublimation temperature, equilibrium vapor pressure, as well as structural properties of this system, are not yet known. Knowledge of these quantities is helpful for the optimization of the conditions for filling carbon nanotubes.

However, the structure of the metallofullerene, $Sc_3N@C_{80}$, has been characterized by ^{13}C and ^{45}Sc NMR [6]. These results indicate that the C_{80} cage possesses I_h symmetry and the encapsulated Sc_3N cluster is not localized at specific bonding sites. In these respects, $Sc_3N@C_{80}$ has a structure similar to that of $La_2@C_{80}$. However, it was found during HPLC studies that $Sc_3N@C_{80}$ elutes with C_{84}-C_{86} cages, and $La_2@C_{80}$ elutes with C_{88}-C_{90} cages [6]. This difference in elution time has been attributed to a decrease of approximately four Pi electrons at the fullerene cage surface relative to $La_2@C_{80}$ and suggests significant electron withdrawal from the carbon cage surface by the central nitrogen atom. Absorption onsets at 1560 nm and 1000 nm were found by UV-Vis/NIR spectroscopy for $La_2@C_{80}$ and $Sc_3N@C_{80}$, respectively. These correspond to bandgaps of 0.8 and 1.3 eV [6].

While the structural characteristics of $La_2@C_{80}$ and $Sc_3N@C_{80}$ are similar, their electronic properties are very different. While it is difficult to estimate the electronic properties of the other members of $Er_xSc_{3-x}N@C_{80}$ (x =0-3), by comparing the filling of SWNTs with these molecules, some insight into the effect of the different charge transfer properties can be achieved. In this paper, the synthesis, structure and high temperature stability of the supramolecular assemblies ($Er_xSc_{3-x}N@C_{80}$@SWNT) are characterized and compared with $La_2@C_{80}$@SWNT.

EXPERIMENTAL

A detailed description of the method by which certain molecules can be inserted into SWNTs is found in our previous works. In this study, $Sc_3N@C_{80}$ was dissolved in toluene, the remaining metallofullerenes were dissolved in carbon disulfide(CS_2). The metallofullerene solution was pipetted dropwise onto a TEM-sized sample of acid-purified SWNT paper synthesized by the arc method [3]. The solvent was allowed to evaporate, and the dry sample was inserted into a JEOL 2010F field emission TEM. The sample was annealed in-situ at 400°C for 10 h at a pressure of ~20-40 μPa. Upon cooling to room temperature, the nanotubes were examined with 97 keV electrons.

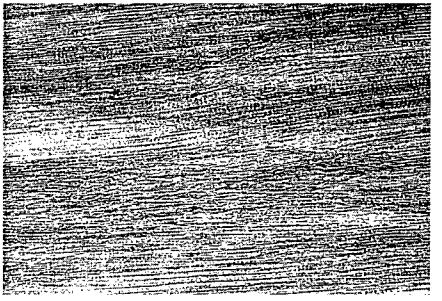

(a)

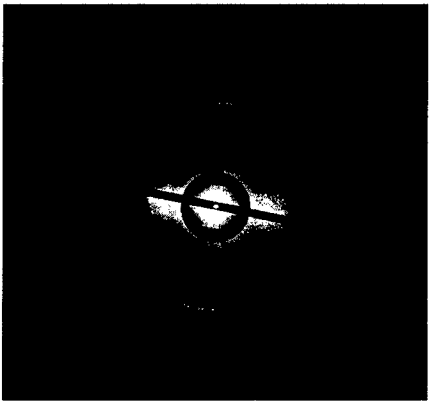

(b)

Figure 1 : (a) $Sc_3N@C_{80}$@SWNT. (b) SAD $Sc_3N@C_{80}$@SWNT

The $Er_xSc_{3-x}N@C_{80}$ (x =0-3) samples were prepared in a similar manner. However, after doping with metallofullerene/CS_2 solution, the samples were placed in a glass ampoule. The ampoule was evacuated under turbo vacuum (10^{-7} torr), the sample was annealed for one hour at 250°C to remove the solvent, and then sealed, all under vacuum. The sealed ampoule with the sample was annealed at 550°C for 44 hours. Upon cooling, the ampoule was broken and the sample was annealed, again, under dynamic vacuum (10^{-7} torr) at 800°C for one hour to remove exterior metallofullerenes. The sample was then cooled, and observed using 97 keV electrons. The $La_2@C_{80}$ sample was prepared in the same manner, however, it was annealed at 600°C for 96 hours.

After being subjected to the above procedure, high temperature experiments were performed via encapsulation under ~10^{-7} torr in a sealed quartz ampoule. Annealing temperatures were 1250°C and 950°C for $Sc_3N@C_{80}$, $La_2@C_{80}$, and $Er_3N@C_{80}$, respectively. The annealing time was 12 hours for each sample.

RESULTS AND DISCUSSION

Efficient filling of SWNTs was achieved for all of the metallofullerenes in this study. In the example in Figure 1a, it is seen that filling of SWNTs with $Sc_3N@C_{80}$ is essentially complete in certain regions of the sample. Each metallofullerene is a weak phase object, whose image is a direct projection of the three dimensional specimen potential in the direction of the electron beam. The images are darkest where the beam propagates through the greatest mass-thickness and is most strongly scattered. Thus, the dark contrast features seen around the edges of the cages are the Sc_3N clusters. There appears to be no organized motion of the endohedral atoms, such as the "ratcheting" that is seen in the case of $La_2@C_{80}$. However, the fact that the clusters are visible under ambient conditions implicates some interaction between the tube and its interior molecules.

Figure 1b shows an electron diffraction (SAD) pattern of a single nanotube rope, abundantly filled with $Sc_3N@C_{80}$, similar to those that appear in Figure 1a. Note that the central area of the pattern is printed at a different contrast scale than the outer area so that

all diffraction features can be more easily seen. This gives rise to a discontinuous contrast artifact where the two areas meet. To facilitate a detailed discussion of the pattern, we begin by defining the meridian and equator as the reciprocal space axes parallel and perpendicular to the predominant direction of the real space rope axis, respectively. The pattern consists of three features: (1) a series of low-Q arcs, centered about the equator (2) a series of high-Q arcs, centered about the meridian, and (3) a series of low-Q reflections, centered about the meridian.

The low-Q equatorial arcs arise from constructive scattering by the planes of SWNTs comprising the rope. The intensity of each arc is greatest at the equatorial axis, reflecting the predominant rope orientation, and subtends an angle corresponding to the mosaic of angular orientations contained within the rope. In other words, the reflections appear as arcs because the rope axis is not perfectly straight over the diffracting area. Due to the small number of lattice planes that comprise the rope, a finite size effect is seen in the form of radial broadening. The reflections are approximately equally spaced in the radial direction, forming a systematic row. This indicates that the rope is not appreciably twisted over the diffracting area such that only one zone axis contributes to the pattern.

The high-Q meridianal arcs arise from constructive scattering by the graphene lattice of each SWNT. The innermost arc corresponds to the graphene (10) reflection at Q ~2.94, and the second arc corresponds to the (11) at Q ~5.09. As with the low-Q equatorial arcs, the intensity profile of the high-Q arcs depend upon rope orientation over the diffracting area and coherence length. However, in this case the chiralities of the constituent tubes must also be considered. For example, consider a spot g located on the (10) arc θ degrees away from the meridian. The intensity at this spot will be the weighted sum of all independent contributions from tubes having (10) scattering that reflect into g. Two extreme cases are achiral (armchair) tubes oriented θ degrees away from the meridian and chiral tubes parallel to the meridian having (10) coherence θ degrees away from the meridian. In this way, the angular intensity profile along each high-Q arc is due to both the mosaic of chiralities and the mosaic of angular orientations of individual SWNTs contained within the rope. Note also that the mosaic of angular orientations within the rope is small, as seen in the small angular broadening of the rope lattice reflections. Thus, high-Q reflections at large azimuthal angles away from the meridian are due to chiral tubes. The corresponding graphene lattice planes have small coherence lengths, resulting in a large degree of radial broadening.

The low-Q meridianal reflections form a systematic row spaced by Q ~0.582, using the graphene lattice reflections that fall on the same axis as a standard for comparison. (This internal calibration is preferred to a more conventional camera length calibration against a known standard because it eliminates measurement errors due to elipticality in the pattern, which would arise if the diffracting rope were slightly tilted out of the object plane.) This Q corresponds to a real space periodicity of ~1.08 nm, equal to the observed periodicity of the encapsulated $Sc_3N@C_{80}$ molecules (c.f. Figure 1a). Similar Q values corresponding to a real space periodicity of ~1.08 nm, have been found for $Er_3N@C_{80}$, $ErSc_2N@C_{80}$ and $La_2@C_{80}$, which is expected given that the symmetry of the C_{80} cage is the same for each. This is consistent with electron diffraction results from C_{60}@SWNT, which shows a fullerene periodicity of 0.98 nm, consistent with the smaller size of the C_{60} molecule.

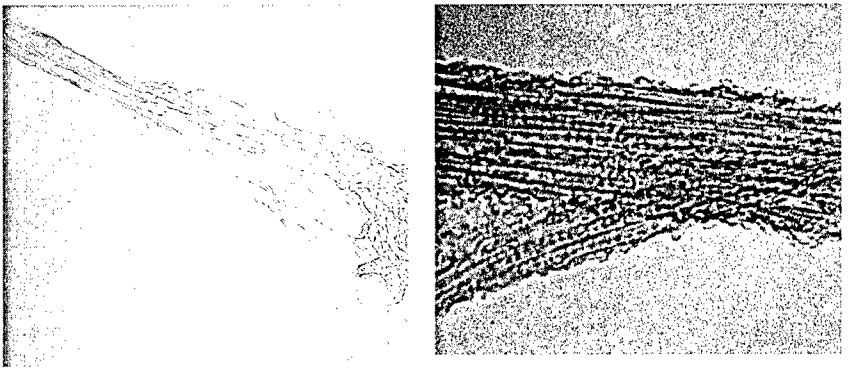

(a) (b)

Figure 2: (a) $La_2@C_{80}$@SWNT at 1250 °C. (b) $Sc_3N@C_{80}$@SWNT at 1250 °C.

The diffraction signature corresponding to the low-Q meridianal reflections are attributed to the periodicity of the C_{80} cages of the encapsulated metallofullerenes. It is possible that the diffraction could be due to the metal clusters themselves. However, the motions of the clusters are both random and independent. It is likely that the metal clusters act only as diffuse scatterers. Our hypothesis is further corroborated by previous diffraction studies of C_{60}@SWNT, which have shown diffraction signatures of 1-D crystals of empty fullerenes.

The materials were annealed at various temperatures between 800°C and 1250°C. Upon observation using HRTEM, prior to high temperature, the samples $La_2@C_{80}$@SWNT and $Er_3N@C_{80}$@SWNT, looked comparable to that of $Sc_3N@C_{80}$@SWNT (c.f. Figure 1a). However, in the $Er_3N@C_{80}$@SWNT sample, some breakdown of the metallofullerenes into co-axial tubes (CATs) was found along with

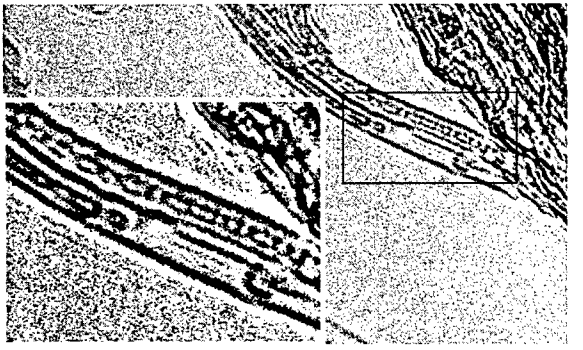

Figure 3: $Er_3N@C_{80}$@SWNT at

peapods. Thus, even relatively mild anneals of 800°C, used during specimen preparation, were sufficient to cause reaction among the $Er_3N@C_{80}$ metallofullerenes. After annealing at 1250°C, the $La_2@C_{80}$@SWNT material was completely transformed into a variety of complex carbon cage structures and multi-wall nanotubes (Figure 2a). The $Sc_3N@C_{80}$@SWNT remained intact (Figure 2b) even though the conditions of the treatment were identical to those of the $La_2@C_{80}$@SWNT sample. After annealing at 950°C, $Er_3N@C_{80}$@SWNT was found to have further CAT formation, as well as remaining peapods. An instance of a unique microstructure was observed in this sample (Figure 3). Micrographs are consistent with a CAT containing intact Er_3N clusters, or a partially transformed structure of covalently bonded metallofullerenes.

The results show a large variation in thermal stability of these C_{80}-based metallofullerenes, even between the isostructural $Er_xSc_{3-x}N@C_{80}$ materials. Variations in electronic properties and interaction with the surrounding SWNT, or cluster mass could be the origin of this behavior. Of particular interest are $La_2@C_{80}$@SWNT and $Sc_3N@C_{80}$@SWNT after annealing at 1250°C. At this temperature, the $Sc_3N@C_{80}$ remains stable, whereas the $La_2@C_{80}$ cages are destroyed. From the variety of reassembled large carbon cage structures in this material, it is apparent that the released La atoms are acting as catalysts for the reformation of the graphitic structures. This interpretation is consistent with the observation of large highly crystalline multi-wall nanotubes which do not exist in the pre-annealed material. The onset of this behavior lies between 1000°C and 1250°C.

The overall response of these supramolecular assemblies to temperature could be affected by the mass of the interior clusters. The heaviest cluster, Er_3N (515.8 g/mol) begins to break down at temperatures below 800°C. The next heaviest metallofullerene with La_2 (277.8 g/mol) has an onset of instability in 1-D clusters at a temperature between 1000°C and 1250°C. The lightest metallofullerene containing Sc_3N (148.9 g/mol) is stable to the highest tested temperature of 1250°C. Thus there is a nominal consistency with cluster mass. This discussion can only be speculative due to the lack of important information on these relatively new metallofullerenes, and other effects could be important in determining thermal stability. For example, it is known that six electrons are transferred to the C_{80} cage from the La atoms in $La_2@C_{80}$. [7] In $Sc_3N@C_{80}$, the electron transfer is two electrons. [6] No data is available for the other C_{80}-based metallofullerenes. These electronic effects could play a key role in determining the stability of the metallofullerenes within the SWNT and governs the strength of interaction and modification of SWNT behavior. This remains for further study.

ACKNOWLEDGEMENTS

The authors gratefully acknowledge the support of the Office of Naval Research through grant N00014-00-1-0482-P00001. This work made use of the central facilities of the University of Pennsylvania, which are supported by the Penn MRSEC under grant NSF DMR00-79909. The authors wish to thank Dr. Patrick Bernier, CNRS, U. Montpellier, and Dr. Pierre Petit, CNRS, Strasbourg for the synthesis and preparation of the acid purified material, respectively.

REFERENCES

1. J.Tang, L.C.Qin, S.Bandow, M.Yudasaka, T.Sasaki, A.Matsushita, S.Iijima, presented at the 2000 MRS Fall Meeting, Boston, MA, 2000 (unpublished).
2. A.Caglar and M.Griebel (private communication).
3. B.W.Smith, D.E.Luzzi, Y.Achiba, Chem. Phys. Lett. **331,** 137 (2000).
4. T.Akasaka, S.Nagase, K.Kobayashi, M.Walchli, K.Yamamoto, H.Funasaka, M.Kako, T.Hoshino, T.Erata , Angew. Chem. Int. Engl. **36**, 1643 (1997).
5. K.Hirahara, K.Suenaga, S.Bandow, H.Kato, T.Okazaki, H.Shinohara, S.Iijima, Phys. Rev. Lett. **85**(25), 5384 (2000).
6. S.Stevenson, G.Rice, T.Glass, K.Harich, F.Cromer, M.R.Jordan, J.Craft, E.Hadju, R.Bible, M.M.Olmstead, K.Maitra, A.J.Fisher, A.L.Balch, H.C.Dorn, Nature **401**, 55 (1999).
7. K.Kobayashi, S.Nagase, T.Akasaka, Chem. Phys. Lett. **245**, 230 (1995).